

# Quasi-SU(3) truncation scheme for even-even *sd*-shell nuclei

C. E. Vargas<sup>1\*</sup>, J. G. Hirsch<sup>2†</sup>, J. P. Draayer<sup>3‡</sup>

<sup>1</sup> Departamento de Física, Centro de Investigación y de Estudios Avanzados del IPN,  
Apartado Postal 14-740 México 07000 DF, México

<sup>2</sup> Instituto de Ciencias Nucleares, Universidad Nacional Autónoma de México,  
Apartado Postal 70-543 México 04510 DF, México

<sup>3</sup> Department of Physics and Astronomy, Louisiana State University,  
Baton Rouge, LA 70803-4001, USA

October 31, 2018

## Abstract

**Abstract** The quasi-SU(3) symmetry was uncovered in full *pf* and *sdg* shell-model calculations for both even-even [1] and odd-even nuclei [2]. It manifests itself through a dominance of single-particle and quadrupole-quadrupole terms in a Hamiltonian used to describe well-deformed nuclei. A practical consequence of the quasi-SU(3) symmetry is an efficient basis truncation scheme. In [3] it is shown that when this type of Hamiltonian is diagonalized in an SU(3) basis, only a few irreducible representations (irreps) of SU(3) are needed to describe the yrast band, the leading S=0 irrep augmented with the leading S=1 irreps in the proton and neutron subspaces. In the present article the quasi-SU(3) truncation scheme is used, in conjunction with a “realistic but schematic” Hamiltonian that includes the most important multipole terms, to describe the energy spectra and B(E2)

---

\*Electronic address: cvargas@fis.cinvestav.mx

†Electronic address: hirsch@nuclecu.unam.mx

‡Electronic address: draayer@lsu.edu

transition strengths of  $^{20,22}\text{Ne}$ ,  $^{24}\text{Mg}$  and  $^{28}\text{Si}$ . The effect of the size of the Hilbert space on both sets of observables is discussed, as well as the structure of the yrast band and the importance of the various terms in the Hamiltonian.

*PACS numbers:* 21.60.Fw, 21.60.Cs, 27.30.+t

*Keywords:* Quasi-SU(3) symmetry, energies, B(E2) values,  $^{20}\text{Ne}$ ,  $^{22}\text{Ne}$ ,  $^{24}\text{Mg}$ ,  $^{28}\text{Si}$ .

## 1 Introduction

More than 40 years ago Elliott pointed out the fundamental role SU(3) plays in a description of light rotational nuclei [4]. The introduction of SU(3) yields insight into relevant degrees of freedom underlying collective rotational motion, and in particular it points to the importance of the quadrupole-quadrupole interaction. Furthermore, even though the spin-orbit interaction breaks SU(3), it can still be used to truncate full model spaces into small subspaces in which realistic calculations can be performed.

In heavy deformed nuclei the pseudo-SU(3) symmetry [5] has played a similar role. While in the 1980s it was employed as an exact symmetry [6, 7, 8, 9], after the development of new computer codes for calculating reduced matrix elements of 1- and 2-body operators [10], it was possible to take into account pseudo-SU(3) symmetry breaking terms in the Hamiltonian (i.e. realistic single-particle energies and the pairing interaction) which have been shown to be important in a description of low-energy bands and associated electromagnetic transition strengths in even-even [11, 12, 13] as well as odd-mass [14, 15] nuclei.

Although the pseudo-SU(3) model is a successful shell-model scheme, it is limited by the formal exclusion of valence nucleons occupying unique parity orbitals. In certain cases a reparametrization of the theory can be used to compensate for this exclusion, while in other cases the nucleons in unique parity orbitals have to be included explicitly [16]. The quasi-SU(3) truncation scheme therefore offers the possibility of including nucleons in intruder orbits within the framework of a complementary SU(3) formalism and thereby yielding a complete theory for heavy deformed nuclei [1].

The quasi-SU(3) symmetry was uncovered in full *pf* and *sdg* shell-model calculations for even-even [1] and odd-even [2] nuclei. It owes its importance

to the dominance of the single-particle and quadrupole-quadrupole terms in a Hamiltonian used to describe well-deformed nuclei. Needless to say, other terms such as pairing are crucial in determining observed moments of inertia, but most of these effects can be accounted for perturbatively because they introduce small changes in the wavefunctions [17].

The quasi-SU(3) symmetry also leads to an efficient truncation scheme. In shell-model calculations it has been shown that the single-particle levels with  $j = l + \frac{1}{2}$  play a dominant role in the low-energy spectra, allowing significant reductions in the size of the Hilbert space [1]. In [3] it is reported that, when a single-particle plus quadrupole-quadrupole Hamiltonian is diagonalized in an SU(3) basis, very few SU(3) irreducible representations (irreps) are needed to describe the yrast band. The ground state band is built from the S=0 leading irrep, which strongly mixes with the leading S=1 irreps in the proton and neutron subspaces. Using a realistic Hamiltonian the change in the wavefunction associated with backbending in  $^{48}\text{Cr}$  was studied in [18].

In the present article the quasi-SU(3) truncation scheme obtained in [3] is used in conjunction with a realistic Hamiltonian. The Hamiltonian has single-particle terms for protons and neutrons, quadrupole-quadrupole and pairing interactions, and three rotor-like terms that allow for a fine tuning of the different bands. The energy spectra and B(E2) transition strength of  $^{20,22}\text{Ne}$ ,  $^{24}\text{Mg}$  and  $^{28}\text{Si}$  are studied. The effects of the size of the Hilbert space on both observables are discussed at length, as well as the yrast band wavefunction and the role played by the different terms in the Hamiltonian.

The main goal is to show that the combination of the quasi-SU(3) truncation scheme and a realistic but simple Hamiltonian is a powerful combination for generating a description of the low-energy properties of deformed nuclei. This work, and a follow-on one where odd-mass and odd-odd light nuclei are discussed [19], provide justification for applications of the quasi-SU(3) truncation scheme to nucleons occupying unique parity orbitals in heavy deformed nuclei.

We study two nuclei, for which a diagonalization in the full Hilbert space in the SU(3) scheme is feasible ( $^{20,22}\text{Ne}$ ), to analyse the effects of the truncation on the energy spectra and B(E2) values. The heavier  $^{24}\text{Mg}$  and  $^{28}\text{Si}$  nuclei have a richer structure and are used to help exhibit the efficiency of the model. The last two nuclei are more affected by the spin-orbit interaction, which introduces significant mixing of SU(3) irreps in the yrast band wavefunction. We will also discuss changes in the rotor-like terms in the Hamiltonian which allow for a best description of the nuclear properties in

each truncated subspace.

The article is organized as follows: In Section 2 a brief review of the SU(3) basis and the model Hamiltonian is presented. Results for  $^{20}\text{Ne}$  are shown and discussed in Section 3, for  $^{22}\text{Ne}$  in Section 4, for  $^{24}\text{Mg}$  in Section 5, and for  $^{28}\text{Si}$  in Section 6. Conclusions are given in Section 7.

## 2 The quasi SU(3) model

There are many articles and books where the SU(3) nuclear model is discussed extensively and to which the interested reader is referred [4, 20, 21, 22, 23, 24]. In the present section we review some properties of the model which are of concern in the present work.

The basis states are written as

$$\{|n_\pi[f_\pi]\alpha_\pi(\lambda_\pi, \mu_\pi), n_\nu[f_\nu]\alpha_\nu(\lambda_\nu, \mu_\nu)\}\rho(\lambda, \mu)kL\{S_\pi, S_\nu\}S; JM\rangle \quad (1)$$

where  $n_\pi$  is the number of valence protons in the  $sd$  shell and  $[f_\pi]$  is the irrep of the U(2) spin group for protons, which has associated with spin  $S_\pi = (f_\pi^1 - f_\pi^2)/2$ . The SU(3) irrep for protons is  $(\lambda_\pi, \mu_\pi)$  with a multiplicity label  $\alpha_\pi$  associated with the reduction from  $U(6)$ . Similar definitions hold for the neutrons, labeled with  $\nu$ . There are other two multiplicity labels:  $\rho$ , which counts how many times the total irrep  $(\lambda, \mu)$  occurs in the direct product  $(\lambda_\pi, \mu_\pi) \otimes (\lambda_\nu, \mu_\nu)$  and  $K$ , which classifies the different occurrences of the orbital angular momentum  $L$  in  $(\lambda, \mu)$ .

The vector states (1) span the complete shell-model space within only one active (harmonic oscillator) shell for each kind of nucleon. As an example, for two protons ( $n_\pi = 2$ ) in the  $sd$  shell there are three possible irreps:  $(\lambda_\pi, \mu_\pi) = (4,0)$ ,  $(2,1)$  and  $(0,2)$ . The first and third irreps have spin zero, the second one has spin 1. Each one occurs only once ( $\alpha_\pi = 1$ ). The same numbers are obtained for 2 neutrons. The coupled SU(3) irreps are ordered by decreasing values of the expectation value of the second order Casimir operator,  $C_2$ ,

$$\langle(\lambda, \mu)|C_2|(\lambda, \mu)\rangle = (\lambda + \mu + 3)(\lambda + \mu) - \lambda\mu. \quad (2)$$

They are listed in Table 1, with the  $(\lambda, \mu)$  labeling the coupled irreps in the third column, the possible values of the total spin  $S$  in the fourth, and the  $C_2$  value in the fifth column.

There is a total of 66 irreps, including the outer multiplicity  $\rho = 1, 2$  in the couplings  $(2, 1)_\pi \otimes (2, 1)_\nu = (3, 1), (1, 2)$ , and the total spin  $S$ . For each

$(\lambda_\pi, \mu_\pi)$	$(\lambda_\nu, \mu_\nu)$	$(\lambda, \mu)$	$S$	$C_2$	$(\lambda_\pi, \mu_\pi)$	$(\lambda_\nu, \mu_\nu)$	$(\lambda, \mu)$	$S$	$C_2$
(4,0)	(4,0)	(8,0)	0	88	(4,0)	(4,0)	(6,1)	0	64
(4,0)	(2,1)	(6,1)	1	64	(2,1)	(4,0)	(6,1)	1	64
(4,0)	(4,0)	(4,2)	0	46	(4,0)	(2,1)	(4,2)	1	46
(2,1)	(4,0)	(4,2)	1	46	(4,0)	(0,2)	(4,2)	0	46
(0,2)	(4,0)	(4,2)	0	46	(2,1)	(2,1)	(4,2)	0,1,2	46
(4,0)	(2,1)	(5,0)	1	40	(2,1)	(4,0)	(5,0)	1	40
(2,1)	(2,1)	(5,0)	0,1,2	40	(4,0)	(4,0)	(2,3)	0	34
(4,0)	(2,1)	(2,3)	1	34	(2,1)	(4,0)	(2,3)	1	34
(2,1)	(2,1)	(2,3)	0,1,2	34	(2,1)	(0,2)	(2,3)	1	34
(0,2)	(2,1)	(2,3)	1	34	(4,0)	(4,0)	(0,4)	0	28
(2,1)	(2,1)	(0,4)	0,1,2	28	(0,2)	(0,2)	(0,4)	0	28
(4,0)	(2,1)	(3,1)	1	25	(2,1)	(4,0)	(3,1)	1	25
(4,0)	(0,2)	(3,1)	0	25	(0,2)	(4,0)	(3,1)	0	25
(2,1)	(2,1)	(3,1)	0,1,2	25	(2,1)	(0,2)	(3,1)	1	25
(0,2)	(2,1)	(3,1)	1	25	(4,0)	(2,1)	(1,2)	1	16
(2,1)	(4,0)	(1,2)	1	16	(2,1)	(2,1)	(1,2)	0,1,2	16
(2,1)	(0,2)	(1,2)	1	16	(0,2)	(2,1)	(1,2)	1	16
(0,2)	(0,2)	(1,2)	0	16	(4,0)	(0,2)	(2,0)	0	10
(0,2)	(4,0)	(2,0)	0	10	(2,1)	(2,1)	(2,0)	0,1,2	10
(2,1)	(0,2)	(2,0)	1	10	(0,2)	(2,1)	(2,0)	1	10
(0,2)	(0,2)	(2,0)	0	10	(2,1)	(2,1)	(0,1)	0,1,2	4
(2,1)	(0,2)	(0,1)	1	4	(0,2)	(2,1)	(0,1)	1	4

Table 1: Complete list of irreps for  $^{20}\text{Ne}$ . The proton  $(\lambda_\pi, \mu_\pi)$ , neutron  $(\lambda_\nu, \mu_\nu)$  and coupled irreps  $(\lambda, \mu)$  are listed in the first three columns, the values of the total spin  $S$  in the fourth, and the  $C_2$  value in the fifth column.

irrep and each spin there are many states, labeled by their orbital angular momentum  $L$ , its multiplicity  $K$ , their total angular momentum  $J$  and its projection  $M$ .

For  $^{20}\text{Ne}$  and  $^{22}\text{Ne}$  all possible states were included. For  $^{24}\text{Mg}$  and  $^{28}\text{Si}$  the space was truncated to allow for faster calculations and to analyze the validity of a truncation scheme based on the quasi-SU(3) basis. The quasi SU(3) truncation scheme is very simple [3]: only the SU(3) irreps with the largest  $\langle C_2 \rangle$  value, in the separate proton and neutron spaces as well as the coupled space, and spin 0 and 1 are included. The inclusion of spin 1 states represents the most important difference from previous SU(3) based truncation schemes [23].

The Hamiltonian of the model is

$$H = H_{sp,\pi} + H_{sp,\nu} - \frac{1}{2} \chi Q \cdot Q - G_\pi H_{pair,\pi} - G_\nu H_{pair,\nu} + a K_J^2 + b J^2 + A_{sym} \tilde{C}_2. \quad (3)$$

The first terms are spherical Nilsson single-particle energies, the quadrupole-quadrupole and pairing interactions. They are the basic components of any realistic Hamiltonian [25, 26] and have been widely studied in the nuclear physics literature, allowing their respective strengths to be fixed by systematics [25, 26]. The remaining are three rotor-like terms used to fine tune the moment of inertia and the position of the different  $K$  bands. The SU(3) mixing is due to the single-particle and pairing terms.

The single-particle part of the Hamiltonian is

$$H_{sp} = \hbar\omega_0 \left( \eta + \frac{3}{2} - 2\kappa \vec{l} \cdot \vec{s} + \kappa\mu \vec{l}^2 \right), \quad (4)$$

with parameters [25]

$$\hbar\omega_0 = 41A^{-1/3}[\text{MeV}], \quad \kappa_\pi = \kappa_\nu = 0.08, \quad \mu_\pi = \mu_\nu = 0.0. \quad (5)$$

The pairing interaction is

$$V_p = -\frac{1}{4}G \sum_{j,j'} a_j^\dagger a_j^\dagger a_{j'} a_{\bar{j}'} \quad (6)$$

where  $\bar{j}$  denotes the time reversed partner of the single-particle state  $j$  and  $G$  is the strength of the pairing force. Its second quantized expression in term

nuclei	Space	$\chi$	$G_{\pi,\nu}$	$A_{sym}$	$a$	$b$
$^{20}\text{Ne}$	full	0.1154	0.4750	0	0.6	-0.010
$^{20}\text{Ne}$	truncated	0.1154	0.4750	0	0.3	0
$^{22}\text{Ne}$	full	0.0984	0.4318	0	0	-0.030
$^{22}\text{Ne}$	truncated	0.0984	0.4318	0.010	0.20	-0.020
$^{24}\text{Mg}$	truncated	0.0851	0.3958	0.08	0.56	0.023
$^{28}\text{Si}$	truncated	0.0658	0.3393	0	0.30	-0.036

Table 2: Parameters of Hamiltonian (3) for the different nuclei listed in the first column. Labels “full” or “truncated” refer to the Hilbert space used.

of SU(3) tensors is reviewed in [23, 15]. The quadrupole-quadrupole ( $\chi$ ) and pairing ( $G_{\pi,\nu}$ ) interaction strengths used are [25, 26]

$$\chi = \frac{17}{A^{5/3}}, \quad G_{\pi} = G_{\nu} = \frac{9.5}{A}. \quad (7)$$

The pairing force parameter (9.5) in these light nuclei ( $A \approx 17 - 28$ ) is about half the one used in heavier nuclei.

The three ‘rotor-like’ terms have been studied in detail in previous papers where the SU(3) and pseudo SU(3) symmetry were used as a dynamical symmetries [7, 8]. In the present work,  $a$  and  $b$  are the two parameters used to fit the spectra.  $A_{sym}$  was used for  $^{22}\text{Ne}$  and  $^{24}\text{Mg}$ . The term proportional to  $K_J^2$  breaks the SU(3) degeneracy of the different K bands [27]. The term proportional to  $J^2$  is used to fine tune the moment of inertia. It represents a small correction to the quadrupole-quadrupole term, which contributes to the rotor spectra with strength  $3/2\chi$  [15]. The symmetry term distinguishes SU(3) irreps with both  $\lambda$  and  $\mu$  even from the others [28], having zero strength in the first case and a positive value in the the second. The net effect of this term is to make contributions of irreps with both  $\lambda$  and  $\mu$  even enhanced relative to the other because they belong to different symmetry types of the intrinsic Vierergruppe  $D_2$  [28].

The values of the Hamiltonian parameters used for the different nuclei are listed in Table 2. The  $a, b$  and  $A_{sym}$  parameters were adjusted to obtain a best fit for each Hilbert space, which is indicated as *full* or *truncated*. In  $^{28}\text{Si}$  we also studied a Hamiltonian with an extra term proportional to the third order Casimir  $C_3$  (see Section 6).

In the following sections we present results for the nuclei  $^{20}\text{Ne}$ ,  $^{22}\text{Ne}$ ,  $^{24}\text{Mg}$  and  $^{28}\text{Si}$ . The effects of both the truncation of the Hilbert space and

the rotor-like terms of the Hamiltonian (3) on the energy spectra and the B(E2) electromagnetic transition strengths are investigated. When possible, a comparison with experimental data [29] and full sd-shell model calculations [30, 31] is given.

### 3 The $^{20}\text{Ne}$ case

$^{20}\text{Ne}$  is considered to be a nucleus with 2 protons and 2 neutrons in the sd-shell, outside an inert  $^{16}\text{O}$  core. The list of the 66 SU(3) irreps that define the full Hilbert space is shown in Table 1.

The energy spectra of  $^{20}\text{Ne}$  obtained with Hamiltonian (3) diagonalized in this basis is shown in the second column of Fig. 1, labeled ‘Full’. A truncated Hilbert space built with only the 12 irreps with the largest  $C_2$  values (listed in the upper six lines in Table 1) was also used. The energy spectra is shown in the first column of Fig. 1, labeled ‘Trunc’. For the full space the rotor parameters were  $A_{sym} = 0, b = -0.01, a = 0.6$  MeV and for the truncated space  $A_{sym} = b = 0, a = 0.3$  MeV. The theoretical results are compared with the experimental energies [29], shown in the third column, and with the energies obtained in previous theoretical studies using an SU(3) basis restricted to S=0 states [24] and the full sd shell-model [31]. In the figure, a) includes the ground state as well as the  $\beta$  and  $\gamma$  bands, while b) shows other excited configurations.

The ground state band ( $0_1^+, 2_1^+, 4_1^+, 6_1^+, 8_1^+$ ) is described almost perfectly by all the models. The  $\gamma$  band, which starts with the  $0_2^+$ , and the  $\beta$  band, which starts with the  $2_2^+$  state, are also described well, however, in the truncated basis their order is reverted. The excited  $4_2^+, 6_2^+, 6_3^+$  are also reproduced well.

The excited  $0_3^+, 0_4^+$  states have energies around 8 MeV. The full basis yields a correct description, while with the truncated space their energies are too high. This is a clear indication of a limitation of the truncated space, namely, it cannot be used to describe highly excited states.

Part b) displays many excited states. While some of them are correctly reproduced, as for example  $2_4^+, 4_3^+, 4_4^+$ , other are not. The  $1^+$  states are some of the worst described. The energies reported in [24], fourth column, are less accurate in their description of some excited states due to the absence of  $S = 1, 2$  states in the basis. It is important to note that even the full space calculation shown in the fifth column does not give a good description of these states.



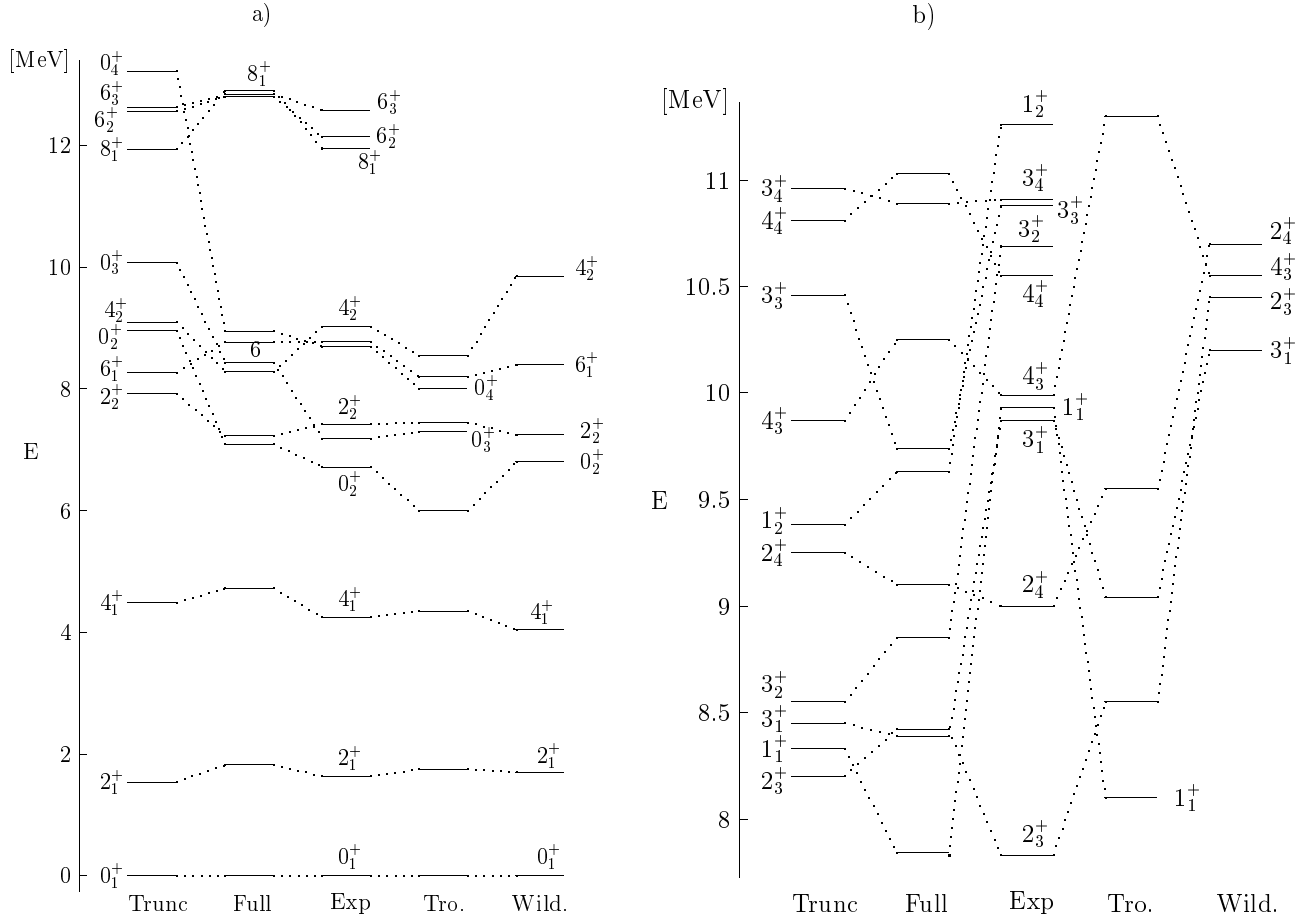


Figure 1: Energy spectra of  $^{20}\text{Ne}$ . For details see the text. The label Tro refers to Ref. [24] and Wild to Ref. [31]. Note that there is a change in scale between a) to b).

$J \rightarrow (J+2)$	Exp.	66	25	17	12	4	1	12*
$0_1 \rightarrow 2_1$	$3.2731 \pm 0.1612$	2.2373	2.3210	2.3802	2.4101	2.5410	2.7312	2.4051
$2_1 \rightarrow 4_1$	$1.2896 \pm 0.1172$	1.0471	1.0302	1.0523	1.0743	1.1424	1.2414	1.0624
$4_1 \rightarrow 6_1$	$0.9316 \pm 0.1397$	0.6594	0.6745	0.6745	0.6802	0.7591	0.8475	0.6670
$6_1 \rightarrow 8_1$	$0.3795 \pm 0.5482$	0.3274	0.3231	0.3261	0.3395	0.3931	0.4527	0.3320
$0_1 \rightarrow 2_7$	$0.0031 \pm 0.0008$	0.0063	0.0353	0.0011	0.0067	0.0033	–	0.0011
$0_2 \rightarrow 2_1$	$0.1177 \pm 0.0145$	0.0948	0.0492	0.0072	0.0074	0.0047	–	0.0072
$0_3 \rightarrow 2_1$	$0.0099 \pm 0.0019$	0.0080	0.0075	0.0227	0.0257	0.0085	–	0.0249
$2_1 \rightarrow 4_8$	$0.0006 \pm 0.0003$	0.0013	0.0001	0.0021	0.0002	0.0001	–	0.0003

Table 3:  $B(E2; J \rightarrow (J+2)) [e^2b^2 \times 10^{-2}]$  transition strengths in  $^{20}\text{Ne}$  for different size model spaces that included the number of  $SU(3)$  irreps indicated on the column header. The last column was obtained with 12 irreps using Hamiltonian parameters that were optimized for that 12-irrep space.

To analyze the effect the truncation of the Hilbert space has on the  $B(E2)$  transition strengths, in Table 3  $B(E2)$  values are shown as a function of the number of  $SU(3)$  irreps included in the basis. These numbers (1, 4, 12, 17, 25, 66) were selected based on changes in the values of  $C_2$  in Table 1, guaranteeing in this way that irreps which contribute with the same intensity to the quadrupole-quadrupole force are all included or all neglected. The first column shows the initial and final angular momentum state of the transition, the second the experimental  $B(E2)$  value, and the remaining six the theoretical  $B(E2)$  values obtained using the same Hamiltonian parameters but reducing the size of the basis (indicated at the top of each column). The last column, labeled 12\*, shows the  $B(E2)$  values obtained using a space with 12 irreps (as for the sixth column) but the Hamiltonian parameters optimized for this space, namely, the same set used to calculate the energy spectra shown in Fig. 1. In all cases an effective charge of  $q_{ef} = 1.558$  was used.

For the  $B(E2)$  transitions within the ground state band any space produces very good results. For the same Hamiltonian parameters, the  $B(E2)$  values all increase as the number of irreps in the basis decreases. The results for 12 irreps with the best-fit parameters are as good as those obtained with the complete basis, and very close to the experimental ones, as can be seen in the first four rows of Table 3.

For  $B(E2)$  transitions from states in excited bands to states in the ground state band the situation changes drastically. The leading irrep is (8,0), which has no  $\gamma$  band. So including only one  $SU(3)$  irrep yields no excited bands and no transitions. The transition  $0_2 \rightarrow 2_1$  is pretty well described with 12

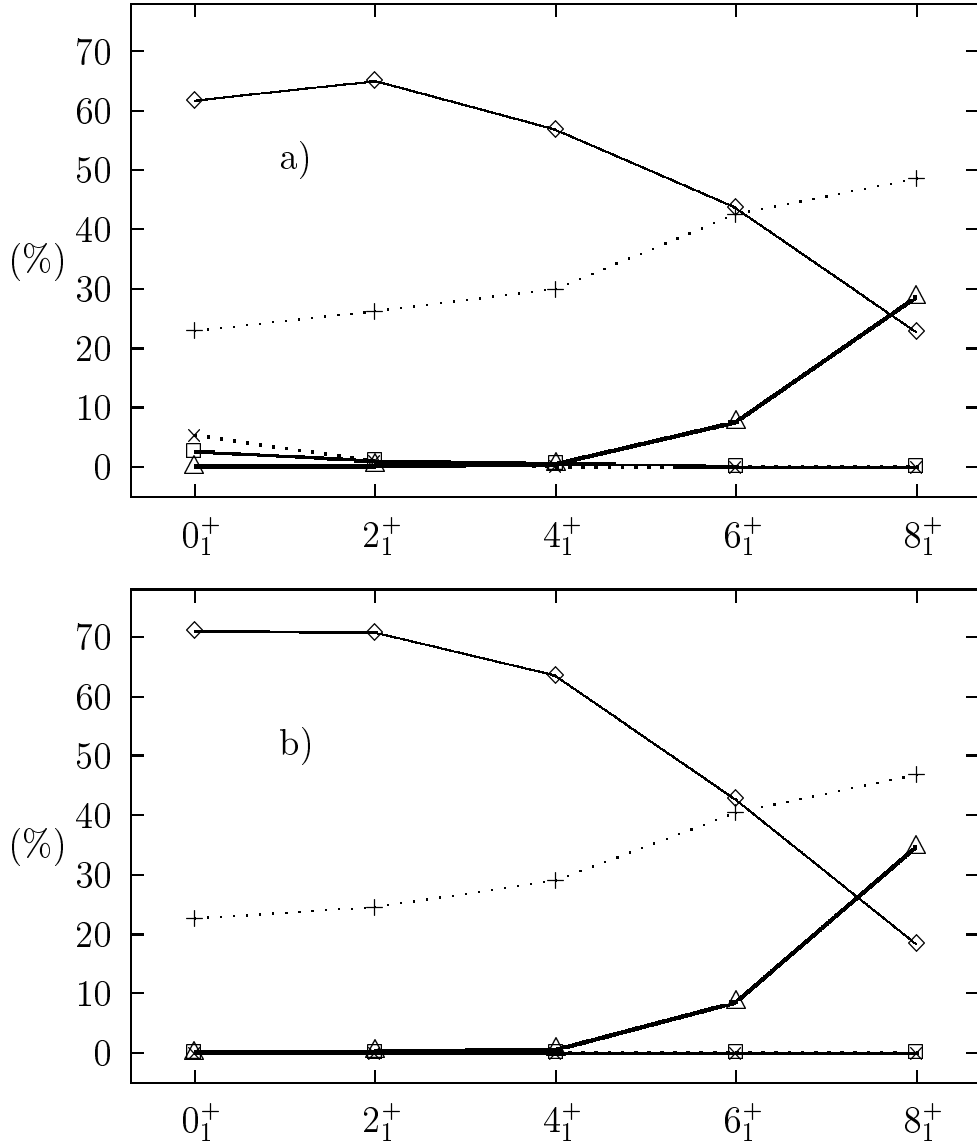


Figure 2: Wavefunction components of states belonging to the ground state band in <sup>20</sup>Ne. The percentage each irrep contributes is shown as a function of the angular momentum for the complete basis, insert a), and the truncated basis, insert b). The convention used is:  $\diamond$  for (8,0)0;  $+$  for (6,1)1;  $\square$  for [(4,0)  $\otimes$  (4,0)] (4,2)0;  $\times$  for [(4,0)  $\otimes$  (0,2)] (4,2)0 and [(0,2)  $\otimes$  (4,0)] (4,2)0; and  $\triangle$  for (4,2)2.

irreps. The  $0_3 \rightarrow 2_1$  transition (next to the last entry in Table 3) is not so well described. The last entry is only reasonable in the complete basis. For basis including 1 or 4 irreps the  $8_1^+$  state always has an energy higher than that observed because the wavefunction is close to a pure rotor. At least 12 irreps are needed to move this state down to the observed energy.

The percentage each SU(3) irrep contributes to the wavefunction of states in the ground state band is shown in Fig. 2 as a function of the angular momentum of each state. Results obtained with the full basis are presented in insert a), and with a basis truncated to 12 irreps in insert b). In both cases the rotor parameters which fit the spectra best were used. It is remarkable that the wavefunctions in the truncated basis are very similar to those obtained using the full basis. This is an important result because even for  $^{20}\text{Ne}$ , the textbook example of a ‘pure’ SU(3) rotor, the leading irrep (8,0) displays very large mixing with the irreps (6,1) with  $S=1$  and, for  $J=8$ , with the irrep (4,2) with  $S=2$ . For  $J=6$  the irrep (8,0) contributes only with 44 %, and for  $J=8$  with 23 %.

The most important conclusion from the  $^{20}\text{Ne}$  results is that while including a few SU(3) irreps in the basis is enough to obtain good wavefunction, irreps with spin 1 and 2 and largest  $C_2$  values must be present. This particular selection of states is what we identify as the *the quasi SU(3) truncation scheme*. This appears to be at work in all the nuclei studied in the present work.

## 4 The $^{22}\text{Ne}$ case

The  $^{22}\text{Ne}$  nucleus has 2 protons and 4 neutrons occupying the sd shell. The proton SU(3) irreps are the same as for  $^{20}\text{Ne}$ . The 4 neutrons can be configured in any one of the 10 irreps listed in Table 4. By coupling the proton and neutron irreps one gets a complete basis, which contains 307 irreps, including the external multiplicity  $\rho$  and all allowed spins. Results are presented in Table 5 for a truncated basis with only the 13 irreps with largest  $C_2$  values. Notice that only proton and neutron irreps with spin 0 and 1 appear in the list (irreps with spin 2 have always a very small  $C_2$  value). These couple to irreps with spin 0, 1 and 2.

The  $^{22}\text{Ne}$  energy spectra is presented in Fig. 3. The first column on the left hand side shows the energies obtained using the truncated basis, the second the energies obtained using the complete basis, the third the

S	irreps
0	(4,2), (0,4), (3,1), (2,0)
1	(5,0), (3,3), (3,1), (1,2), (0,1)
2	(1,2)

Table 4: SU(3) irreps for 4 particles in the sd-shell.

$(\lambda_\pi, \mu_\pi)$	$(\lambda_\nu, \mu_\nu)$	$(\lambda, \mu)$	$S$	$C_2$	$(\lambda_\pi, \mu_\pi)$	$(\lambda_\nu, \mu_\nu)$	$(\lambda, \mu)$	$S$	$C_2$
(4,0)	(4,2)	(8,2)	0	114	(4,0)	(5,0)	(9,0)	1	108
(4,0)	(4,2)	(6,3)	0	90	(4,0)	(2,3)	(6,3)	1	90
(2,1)	(4,2)	(6,3)	1	90	(4,0)	(4,2)	(7,1)	0	81
(4,0)	(5,0)	(7,1)	1	81	(4,0)	(3,1)	(7,1)	0	81
(4,0)	(3,1)	(7,1)	1	81	(2,1)	(4,2)	(7,1)	1	81
(2,1)	(5,0)	(7,1)	0	81	(2,1)	(5,0)	(7,1)	1	81
(2,1)	(5,0)	(7,1)	2	81					

Table 5: List of irreps included in the truncated basis for  $^{22}\text{Ne}$ . The proton  $(\lambda_\pi, \mu_\pi)$ , neutron  $(\lambda_\nu, \mu_\nu)$  and coupled irreps  $(\lambda, \mu)$  are listed in the first three columns, the values of the total spin  $S$  in the fourth, and the  $C_2$  value in the fifth column.

experimental energies [29] and the fourth the energies obtained using full *sd*-shell model calculations [30]. Insert a) displays the ground state and  $\beta$  bands, insert b) other excited bands. The ground state and the  $\beta$  bands are very well described with both the complete and the truncated basis. Other states like  $1_1^+$ ,  $3_1^+$ ,  $4_2^+$ ,  $3_2^+$ ,  $0_2^+$  and  $4_3^+$  are also reasonable well predicted. In contrast, for a number of highly excited states ( $5_1^+$ ,  $1_2^+$ ,  $6_2^+$ ,  $0_3^+$ ,  $0_4^+$ ) the model fails when the truncated basis is used. This is particularly so for the states  $2_4^+$ ,  $1_2^+$ ,  $0_3^+$  and  $0_4^+$ . Nonetheless, the overall description of  $^{22}\text{Ne}$  is quite good.

As was seen for the  $^{20}\text{Ne}$  case, the single particle energies together with the pairing and quadrupole-quadrupole interactions suffices to reproduce the gross features of the energy spectrum. Small corrections are introduced by the rotor-like terms ( $K^2$  for  $^{20}\text{Ne}$ ,  $J^2$  for  $^{22}\text{Ne}$ ), which allow for a fine tuning of the energies. This is another very important result. It reflects on the fact that the Hamiltonian parameters taken from systematics are quite good, allowing a description comparable to the *sd*-shell model. When coupled with the truncation scheme outlined above, they constitute the main ingredients of a powerful and predictive model, the quasi-SU(3) scheme.

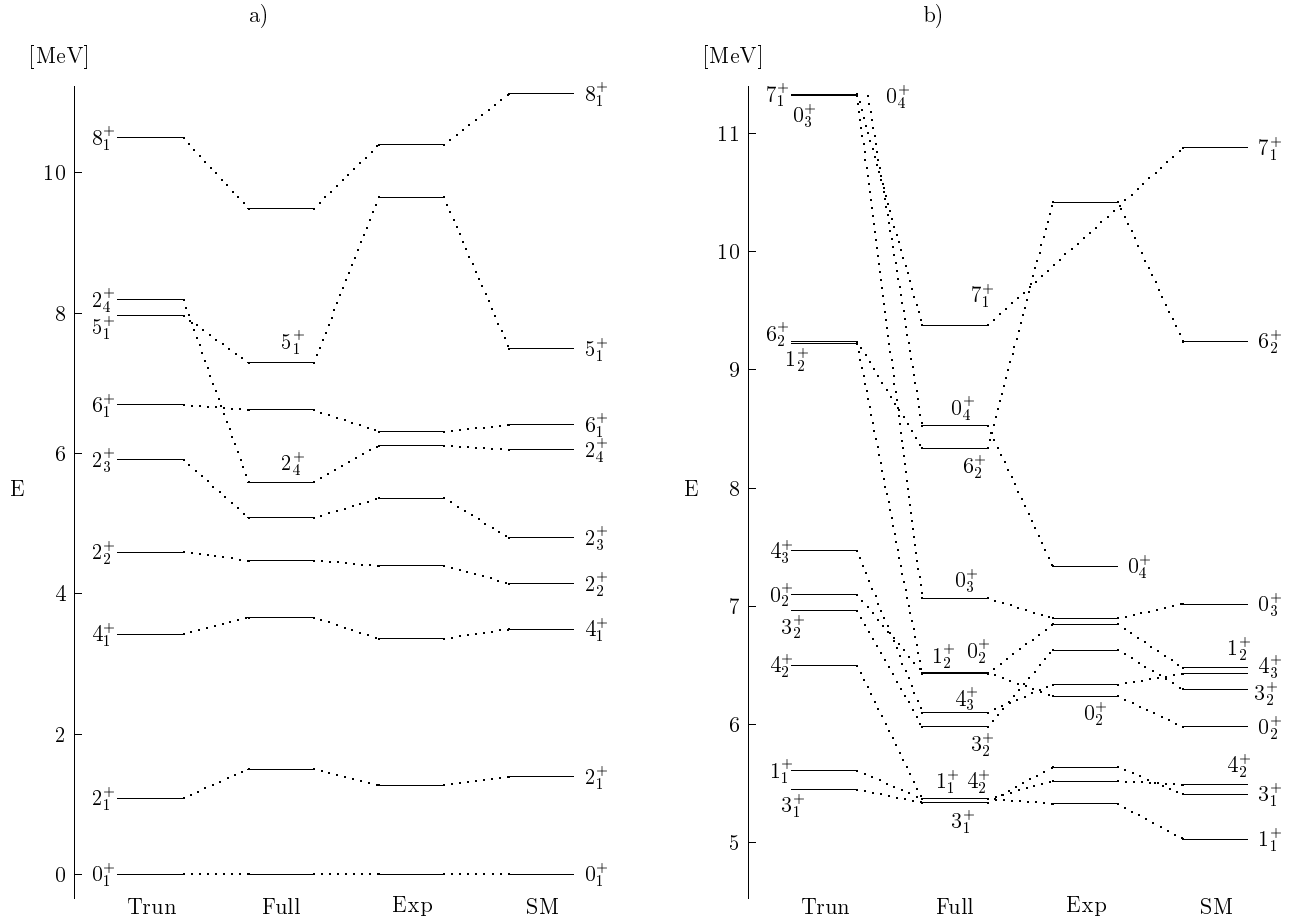


Figure 3: Energy spectra of  $^{22}\text{Ne}$ . Insert a) shows the ground and  $\gamma$  bands, insert b) other excited bands. Experimental energies are displayed in the third column, theoretical results obtained using the truncated basis in the first column and with the complete basis in the second column. Fourth column displays the shell-model results [30].

$J \rightarrow (J + 2)$	Experimental	Truncated	Complete
$0_1 \rightarrow 2_1$	$2.2886 \pm 0.0915$	2.3192	2.0925
$2_1 \rightarrow 4_1$	$1.1650 \pm 0.0265$	1.0684	0.9419
$4_1 \rightarrow 6_1$	$0.7245 \pm 0.0898$	0.7628	0.6402
$6_1 \rightarrow 8_1$		0.4931	0.2885
$0_1 \rightarrow 2_2$	$> 0.0476$	0.0241	0.0222
$2_1 \rightarrow 4_2$	$0.0062 \pm 0.0015$	0.0008	0.0024
$2_2 \rightarrow 4_2$		0.4489	0.0971
$4_2 \rightarrow 6_2$		0.5624	0.2073
$6_2 \rightarrow 8_2$		0.3639	0.1656

Table 6:  $B(E2; J \rightarrow (J+2)) [e^2b^2 \times 10^{-2}]$  transition strengths for  $^{22}\text{Ne}$ . Experimental and theoretical values, both for the truncated and the complete basis, are shown in columns 2, 3 and 4 respectively.

The  $^{22}\text{Ne}$   $B(E2)$  transition strengths are presented in Table 6. The theoretical results obtained with  $q_{eff} = 1.3$  agree well with the known experimental data (there are three strengths measured between states in the ground state band as well as two transitions between bands). As was the case for  $^{20}\text{Ne}$ , the  $B(E2)$  transition strengths between members of the ground state band are pretty well described within both the truncated and the complete Hilbert space, while the transitions between states in gamma bands differ, with the complete space predictions being smaller.

The ground state wavefunctions obtained using the complete and truncated bases are displayed in Fig. 4 as a function of the angular momentum of the states. While the details may differ, a comparison of the wavefunctions exhibit the same trends in both the complete and truncated basis. For  $J=0$  the irrep  $(4,0)_\pi \otimes (4,2)_\nu \rightarrow (8,2)$   $S=0$  dominates, with significant mixing with the irreps  $(9,0)$   $S=1$ ,  $(6,3)$   $S=1$  and  $(7,1)$   $S=1$ . For larger values of the angular momentum, the contribution of the irrep  $(8,2)$   $S=0$  decreases, being replaced by the irrep  $(7,1)$   $S=2$  for  $J = 8$  and  $10$ . The important role played by the  $SU(3)$  irreps with spin  $S = 1$  and  $2$  in the ground state band is the most significant departure from the usual Elliot  $SU(3)$  symmetry and, as mentioned above, is the manifestation of the quasi- $SU(3)$  symmetry.

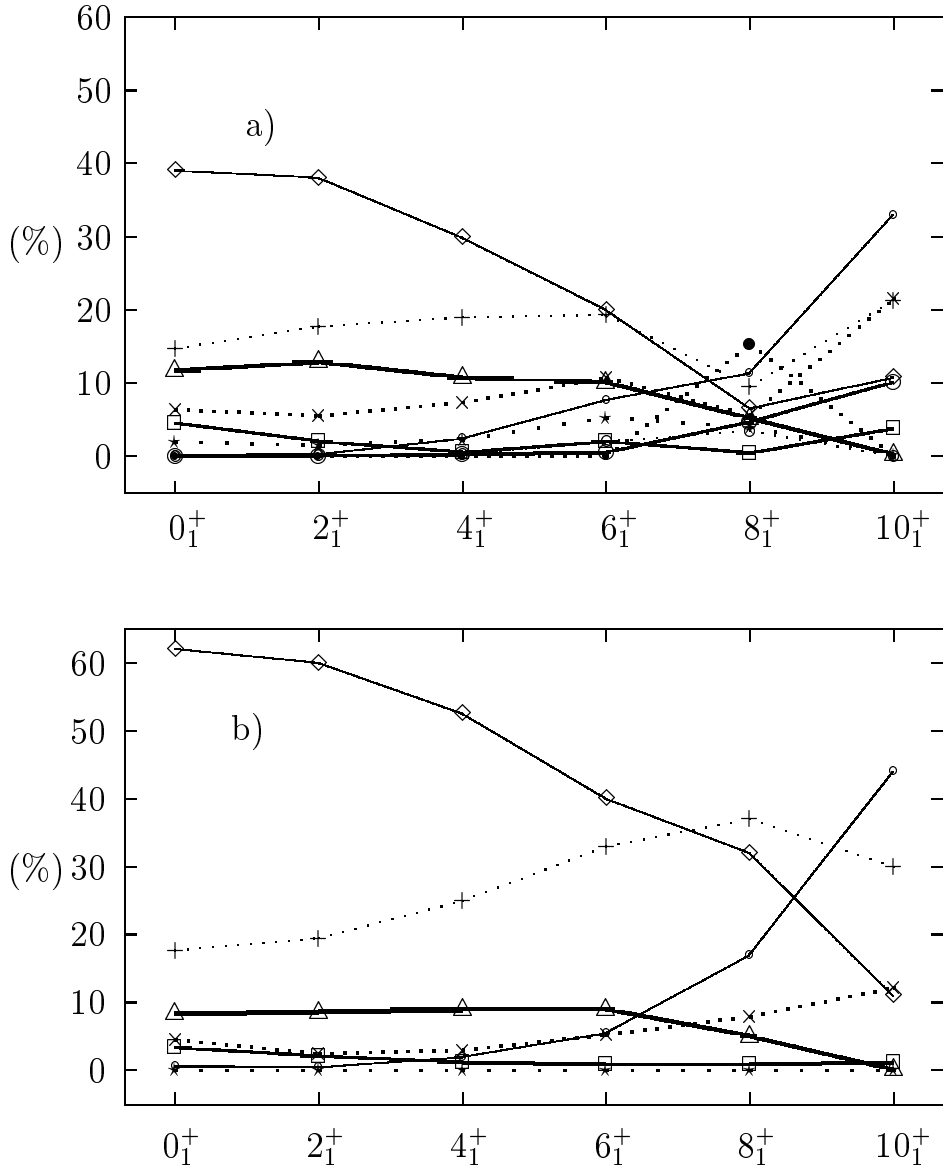


Figure 4: Wavefunction components of states belonging to the ground state band in  $^{22}\text{Ne}$ . The percentage each irrep contributes to the wavefunction is shown as function of the angular momentum for the complete basis, insert a) and the truncated basis, insert b). The convention used is:  $\diamond$  for  $(8,2)0$ ;  $+$  for  $(9,0)1$ ;  $\square$  for  $[(4,0) \otimes (2,3)] (6,3)1$ ;  $\times$  for  $[(2,1) \otimes (4,2)] (6,3)1$ ;  $\triangle$  for  $[(4,0) \otimes (3,1)] (7,1)1$ ;  $\star$  for  $[(2,1) \otimes (4,2)] (7,1)1$ ;  $\circ$  for  $(7,1)2$ ;  $\odot$  for  $(6,0)2$ ;  $\bigcirc$  for  $(4,4)2$ ; and  $\bullet$  for  $(5,2)2, (3,3)2,3$ .



$(\lambda_\pi, \mu_\pi)$	$(\lambda_\nu, \mu_\nu)$	$(\lambda, \mu)$	$S$	$C_2$	$(\lambda_\pi, \mu_\pi)$	$(\lambda_\nu, \mu_\nu)$	$(\lambda, \mu)$	$S$	$C_2$
(4,2)	(4,2)	(8,4)	0	148	(4,2)	(4,2)	(9,2)	0	136
(4,2)	(5,0)	(9,2)	1	136	(5,0)	(4,2)	(9,2)	1	136
(4,2)	(4,2)	(10,0)	0	130	(5,0)	(5,0)	(10,0)	0	130
(5,0)	(5,0)	(10,0)	1	130	(5,0)	(5,0)	(10,0)	2	130
(4,2)	(4,2)	(6,5)	0	124	(4,2)	(2,3)	(6,5)	1	124
(2,3)	(4,2)	(6,5)	1	124					

Table 7: List of irreps included in the truncated basis for  $^{24}\text{Mg}$ . The proton  $(\lambda_\pi, \mu_\pi)$ , neutron  $(\lambda_\nu, \mu_\nu)$  and coupled irreps  $(\lambda, \mu)$  are listed in the first three columns, the values of the total spin  $S$  in the fourth, and the  $C_2$  value in the fifth column.

## 5 The $^{24}\text{Mg}$ case

The  $^{24}\text{Mg}$  nucleus has four protons and four neutrons in the active sd shell. The 10 SU(3) irreps for protons and neutrons are those listed in Table 4. The complete basis includes 1599 irreps, taking into account the external multiplicity  $\rho$  and the different spin values. Calculations were carried out in truncated Hilbert space built with the 11 SU(3) irreps listed in Table 7. Again, these are the SU(3) irreps with the largest  $C_2$  value. Proton and neutron irreps either spin  $S=0$  and 1 and the coupled irreps have spin  $S = 0, 1$  and 2.

As can be seen in Table 2, the Hamiltonian parameters include an symmetry parameter. This is required to lower the energy of the  $8_1^+$  state, which is a member of the ground state band. The energy spectra of  $^{24}\text{Mg}$  is shown in Fig. 5. The first column displays the shell-model values, the second the experimental data, and the third the predicted energies in the truncated basis. The last three columns show the effect on the spectra of turning off the  $K^2$  term ( $a = 0$ ), both the  $K^2$  and the symmetry term ( $a = A_{sym} = 0$ ) and the three rotor terms ( $a = b = A_{sym} = 0$ ), respectively.

The present theoretical spectra ('Trun') reproduce the observed energy levels and the full shell-model calculations fairly well. As mentioned above, gross features of the spectra are reproduced by the dominant terms in Hamiltonian (3): the single particle, pairing and quadrupole-quadrupole interactions, whose strength are fixed from systematics. The spectra obtained with no rotor-like terms is shown in the last column (right hand side) of Fig. 5. The ordering of the levels is correct, with only one crossing of two neighboring

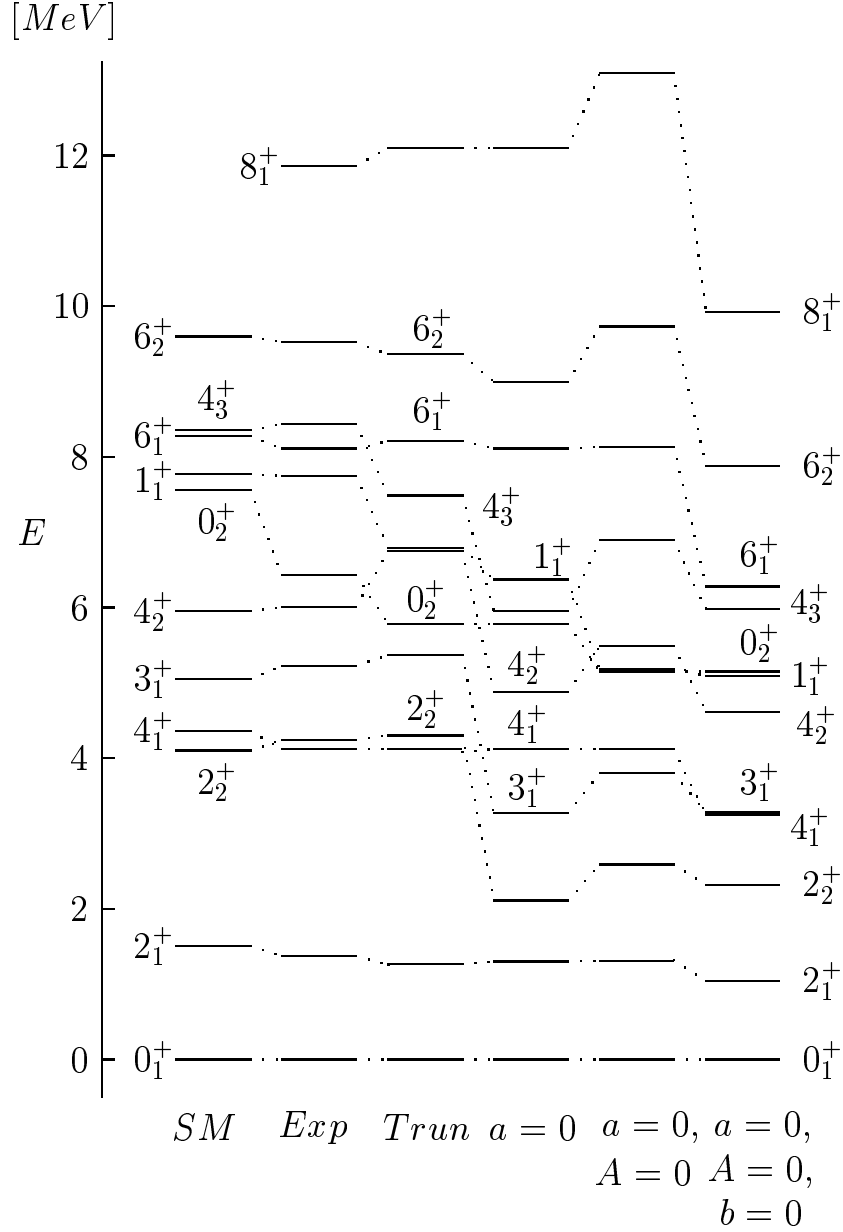


Figure 5: Energy spectra of  $^{24}\text{Mg}$ . The first column displays the full shell-model values, the second one the experimental data, the third the predicted energies in the truncated basis. The last three columns show the effect on the energy spectra of turning off the  $K^2$  term ( $a = 0$ ), both the  $K^2$  and the symmetry term ( $a = A_{sym} = 0$ ) and the three rotor terms ( $a = b = A_{sym} = 0$ ), respectively. The *SM* values were taken from [31, 32].

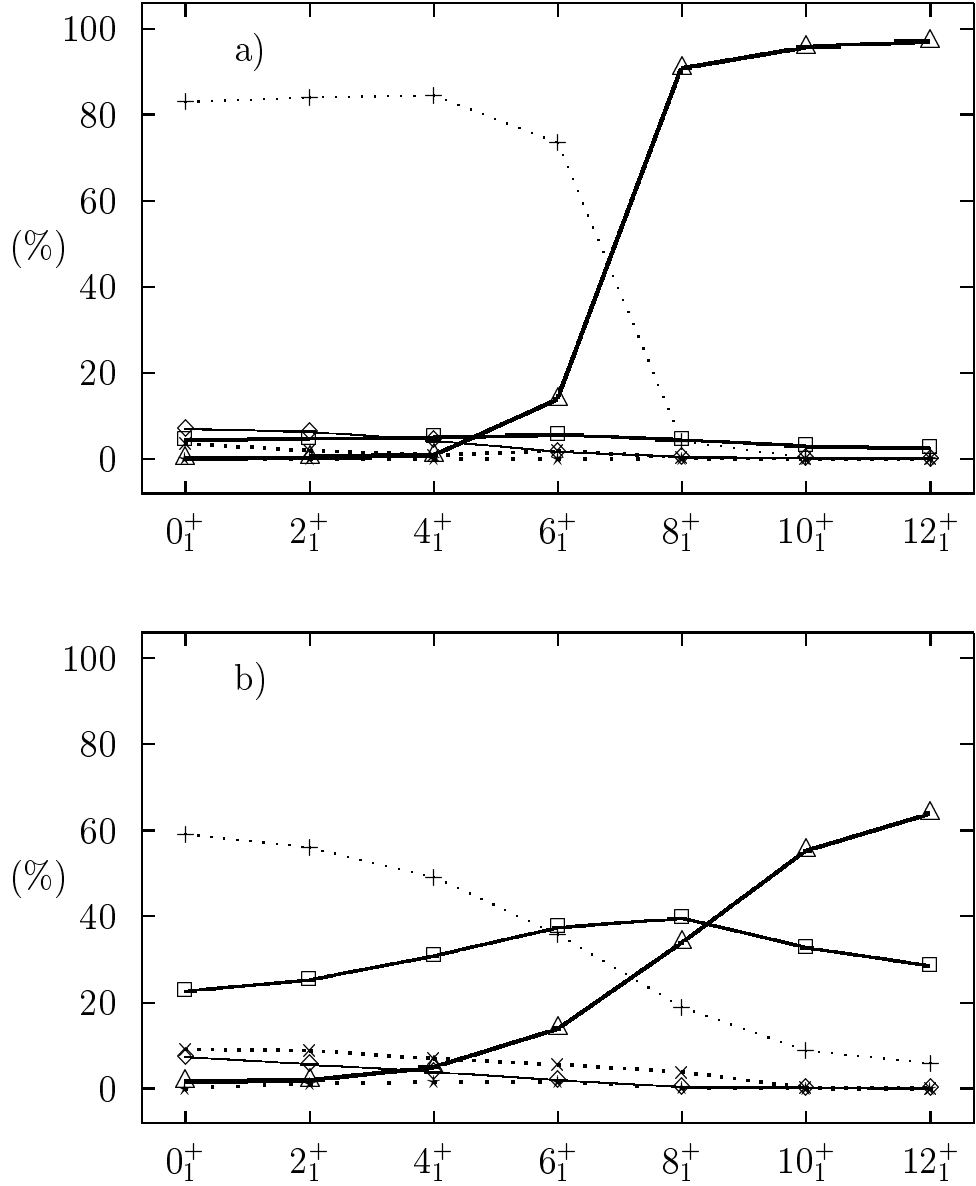


Figure 6: Wave function composition of states in the ground state band of  $^{24}\text{Mg}$  as a function of their angular momentum. Insert a) shows the results using the complete Hamiltonian (3), insert b) the results setting  $a = b = A_{sym} = 0$ . The percentage each irrep contributes is shown on the vertical axis. The convention used is  $\diamond$  for  $(10,0)0$ ; + for  $(8,4)0$ ;  $\square$  for  $(9,2)1$ ;  $\times$  for  $(6,5)1$ ;  $\triangle$  for  $(10,0)2$ ; and  $\star$  for  $(10,0)0$ .

$J \rightarrow (J + 2)$	Experimental	Theoretical
$0_1^+ \rightarrow 2_1^+$	$4.3588 \pm 0.1028$	4.7742
$2_1^+ \rightarrow 4_1^+$	$2.6915 \pm 0.3738$	2.3138
$4_1^+ \rightarrow 6_1^+$	$2.3165 \pm 0.8316$	1.7052
$6_1^+ \rightarrow 8_1^+$		0.5366
$8_1^+ \rightarrow 10_1^+$		1.1093
$10_1^+ \rightarrow 12_1^+$		0.6164
$0_1^+ \rightarrow 2_2^+$	$0.3310 \pm 0.0226$	0.5022
$0_1^+ \rightarrow 2_3^+$	$0.1172 \pm 0.0514$	0.0004
$0_2^+ \rightarrow 2_1^+$	$0.0214 \pm 0.0033$	0.0005
$0_2^+ \rightarrow 2_2^+$	$0.2919 \pm 0.0493$	0.0590
$0_2^+ \rightarrow 2_3^+$		3.2228
$0_2^+ \rightarrow 2_4^+$	$2.6729 \pm 1.0280$	1.3583
$2_1^+ \rightarrow 4_2^+$	$0.0733 \pm 0.0052$	0.0531
$2_1^+ \rightarrow 4_3^+$	$0.0747 \pm 0.0299$	0.0075
$2_1^+ \rightarrow 4_4^+$	$0.0254 \pm 0.0075$	0.0045
$2_2^+ \rightarrow 4_2^+$	$0.9495 \pm 0.0822$	0.8766
$2_2^+ \rightarrow 4_3^+$	$0.0972 \pm 0.0448$	0.0067
$2_2^+ \rightarrow 4_4^+$	$0.0067 \pm 0.0029$	0.0007
$2_3^+ \rightarrow 4_3^+$	$2.9159 \pm 1.1962$	1.5760
$2_3^+ \rightarrow 4_4^+$	$2.1681 \pm 0.6729$	0.6478
$4_1^+ \rightarrow 6_2^+$	$0.0356 \pm 0.0178$	0.1167
$4_2^+ \rightarrow 6_2^+$	$1.0691 \pm 0.5346$	0.0058
$6_1^+ \rightarrow 8_2^+$		0.8532
$6_2^+ \rightarrow 8_1^+$		1.0034
$6_2^+ \rightarrow 8_2^+$		0.4719

Table 8: B(E2) transition strengths for  $^{24}\text{Mg}$  (in  $[e^2b^2 \times 10^{-2}]$ ).  $q_{eff}$  is 1.6.

levels:  $1_1^+$  and  $4_2^+$ . The first  $2^+$  state is about at the right energy. However, without the rotor-like terms the model fails to reproduce the moment of inertia of the ground state band, the energy of the  $\gamma$  band head and other features. The energy of the state in the  $\gamma$  band is substantially controlled by the  $K^2$  term. This is why it was introduced [27]. Without only this term the  $\gamma$  band energies are clearly depressed, as seen in the third column. The most prominent effect of not including the symmetry term is in the energy of the  $8_1^+$  state. This term reduces the mixing of the leading irrep (8,4)  $S = 1$  with other irreps which have  $\lambda$  or  $\mu$  odd, a mixing that is driven by the single particle terms of the Hamiltonian. It was also noted in a study of the mapping of the rotor to the SU(3) model [28]. It is shown here to contribute to the correct prediction of the energies of high energy states belonging to the ground state band.

Fig. 6 shows the percentage each irrep contributes to the wavefunction of states in the ground state band of  $^{24}\text{Mg}$  as a function of their angular momentum. The upper panel shows the results using the complete Hamiltonian (3), the lower panel the results of setting  $a = b = A_{sym} = 0$ . The introduction of the symmetry term strongly diminishes the mixing. There is a sudden change in the wavefunction from  $J=6$  to  $J=8$ , where the dominance of the (8,4)  $S=0$  irrep is replaced by the (10,0)  $S=2$ . This change in the spin contribution to states in the ground state band was also found in full shell-model calculations of  $^{24}\text{Mg}$  [33].

Calculations were performed also for other basis sets, containing 1, 4, 8, 26, 34, 54, and 62 irreps. In all cases similar fits were found, with the parameter  $b$  ranging between 0.01 and 0.03 and  $A_{sym}$  between 0.04 and 0.08.

The B(E2) transition strengths for  $^{24}\text{Mg}$  are listed in Table 8. Experimental values are shown in the second column. Theoretical values were calculated using an effective charge  $q_{eff} = 1.6$  and are displayed in the third column. The overall agreement is reasonable. The change in the wavefunction of the  $8_1^+$  state reflects in a fragmentation of the B(E2) strengths between the transitions  $6_1^+ \rightarrow 8_1^+$  and  $6_1^+ \rightarrow 8_2^+$ . None of these have been measured.

## 6 The $^{28}\text{Si}$ case

The  $^{28}\text{Si}$  nucleus has 6 protons and 6 neutrons occupying the sd shell. Six like particles in the  $sd$ -shell populate the 15 irreps listed with their spin  $S$  in Table 9.

S	irreps
0	(6,0), (0,6), (3,3), (2,2), (0,0)
1	(3,3), (4,1), (1,4), (2,2), (3,0), (0,3), (1,1)
2	(2,2), (1,1)
3	(0,0)

Table 9: SU(3) irreps for 6 particles in the sd shell.

$(\lambda_\pi, \mu_\pi)S_\pi$	$(\lambda_\nu, \mu_\nu)S_\nu$	$(\lambda, \mu)$	$S$	$C_2$	$(\lambda_\pi, \mu_\pi)S_\pi$	$(\lambda_\nu, \mu_\nu)S_\nu$	$(\lambda, \mu)$	$S$	$C_2$
(6,0)0	(6,0)0	(12,0)	0	180	(0,6)0	(0,6)0	(0,12)	0	180
(6,0)0	(3,3)0	(9,3)	0	153	(6,0)0	(3,3)1	(9,3)	1	153
(0,6)0	(3,3)0	(3,9)	0	153	(0,6)0	(3,3)1	(3,9)	1	153
(3,3)0	(6,0)0	(9,3)	0	153	(3,3)1	(6,0)0	(9,3)	1	153
(3,3)0	(0,6)0	(3,9)	0	153	(3,3)1	(0,6)0	(3,9)	1	153
(6,0)0	(6,0)0	(10,1)	0	144	(6,0)0	(0,6)0	(6,6)	0	144
(0,6)0	(6,0)0	(6,6)	0	144	(0,6)0	(0,6)0	(1,10)	0	144
(6,0)0	(4,1)1	(10,1)	1	144	(4,1)1	(6,0)0	(10,1)	1	144
(0,6)0	(1,4)1	(1,10)	1	144	(1,4)1	(0,6)0	(1,10)	1	144
(3,3)0	(3,3)0	(6,6)	0	144	(3,3)1	(3,3)1	(6,6)	0	144
(3,3)1	(3,3)1	(6,6)	1	144	(3,3)1	(3,3)1	(6,6)	2	144
(3,3)0	(3,3)1	(6,6)	1	144	(3,3)1	(3,3)0	(6,6)	1	144

Table 10: List of irreps included in the truncated basis for  $^{28}\text{Si}$ . The proton  $(\lambda_\pi, \mu_\pi)$  and neutron  $(\lambda_\nu, \mu_\nu)$  irreps with their spins  $S_\pi$  and  $S_\nu$ , and coupled irreps  $(\lambda, \mu)$  are listed in the first three columns, the values of the total spin  $S$  in the fourth, and the  $C_2$  value in the fifth column.

The complete basis includes 4045 irreps, taking into account the external multiplicity  $\rho$  and the different spin values. Calculations were carried out in a severely truncated Hilbert space, built with the 24 SU(3) irreps listed in Table 10. Again, these are the SU(3) irreps with the largest  $C_2$  values. As in previous cases, proton and neutron irreps include those with spin  $S = 0$  and 1, while total irreps have spin  $S = 0, 1$  and 2. The proton and neutron spin  $S_\pi, S_\nu$  are shown explicitly in order to distinguish the irreps (3,3) with spin  $S = 0$  and 1.

The  $^{28}\text{Si}$  energy spectra is shown in Fig. 7. It was obtained with the parametrization given in Table 2 for the Hamiltonian (3) plus a term proportional to  $C_3$ , the third order SU(3) Casimir operator. The  $C_3$  eigenvalues

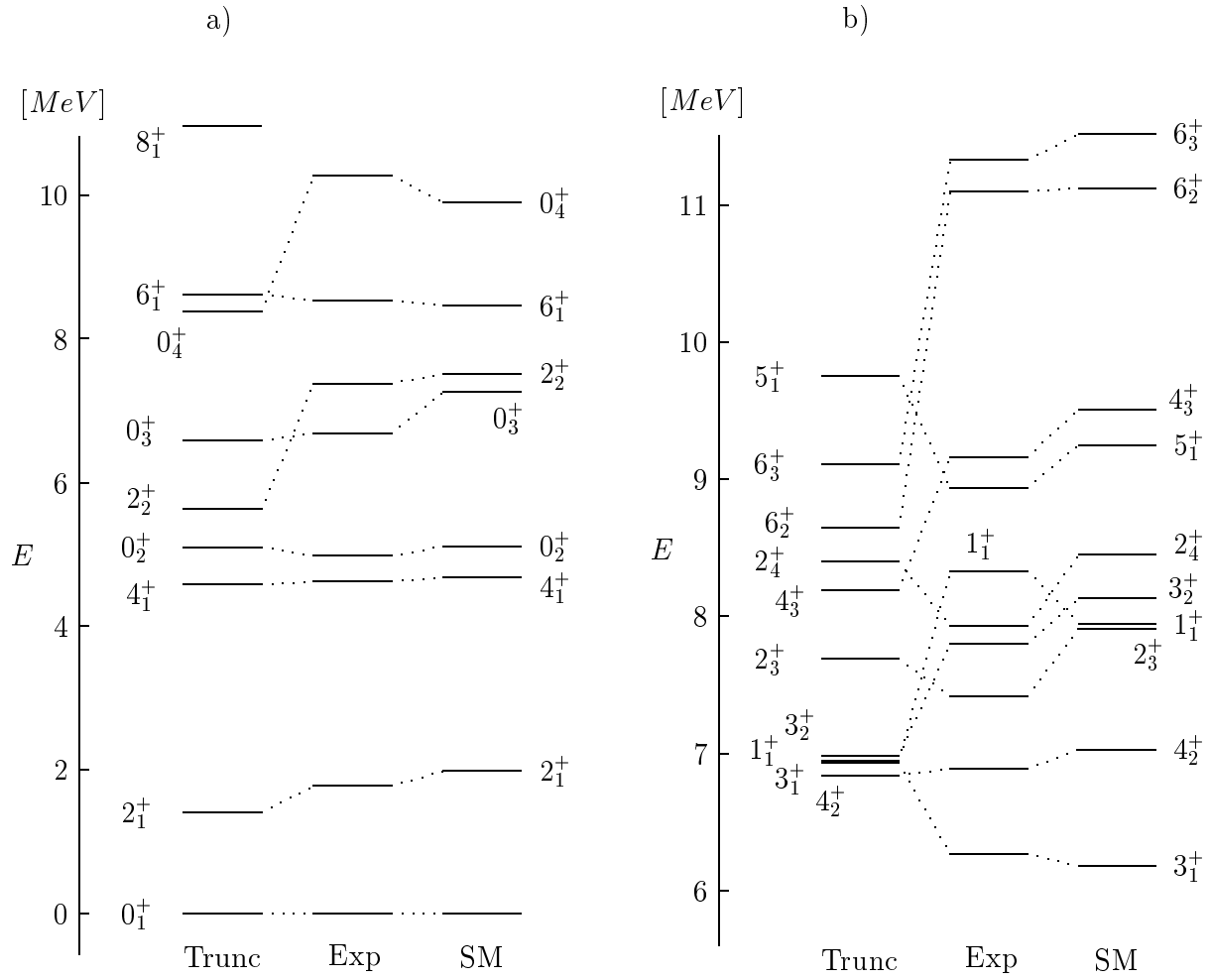


Figure 7: Energy spectra for  $^{28}\text{Si}$ . Experimental results are shown in the first column, theoretical energies calculated with the present model are displayed in the second column, and those obtained with a full shell model calculation [31, 32] in the third.

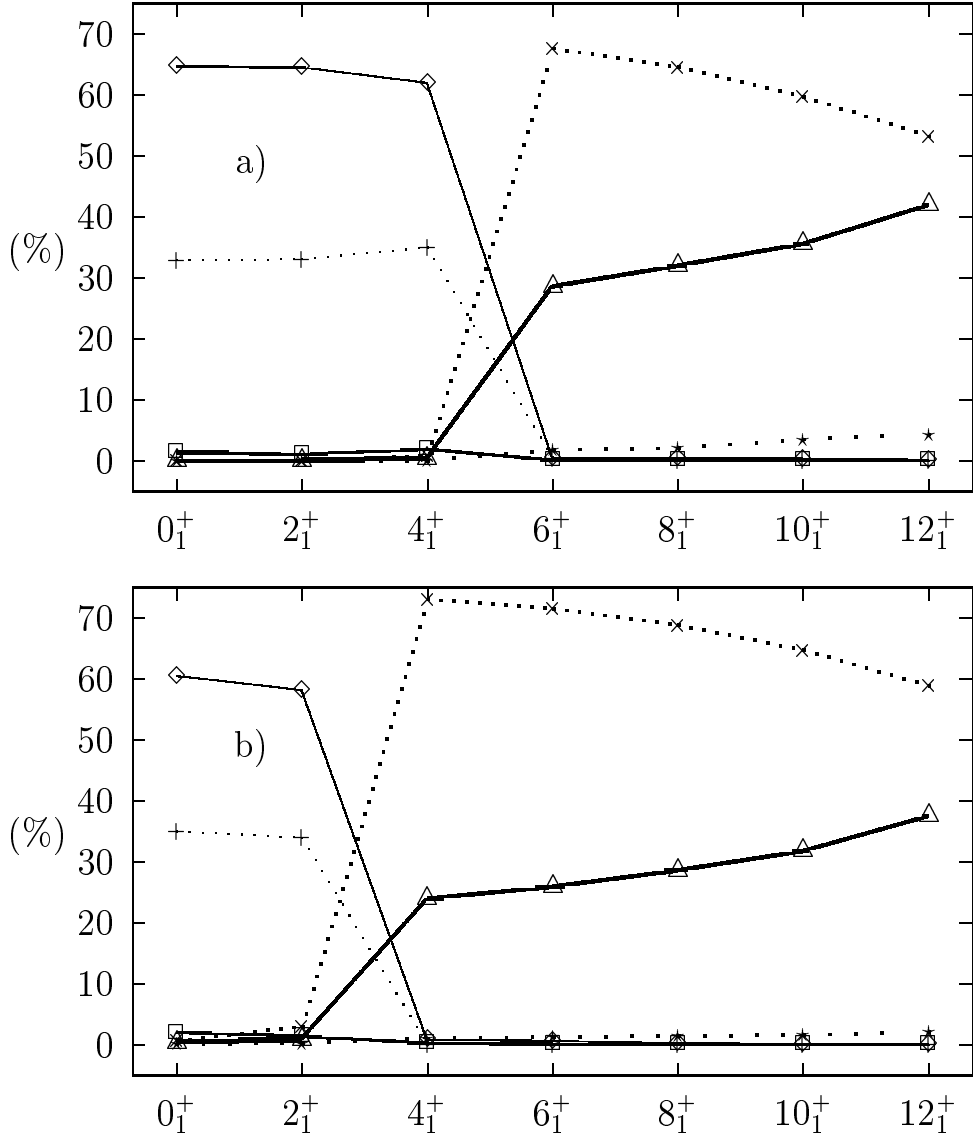


Figure 8: Wavefunction components of states belonging to the ground state band in  $^{28}\text{Si}$ . The percentage each irrep contributes is shown as a function of the angular momentum for the basis with 24 irreps, in insert a) with the Hamiltonian shown in Table 2 plus the  $C_3$  term and insert b) for the same Hamiltonian but without  $C_3$ . The convention used is  $\diamond$  for (0,12)0; + for (1,10)1;  $\square$  for (12,0)0,  $\times$  for (10,1)0,  $\triangle$  for (2,8)2, and  $\star$  for (8,2)2.



$J \rightarrow (J + 2)$	Experimental	Theoretical
$0_1^+ \rightarrow 2_1^+$	$3.3334 \pm 0.0757$	4.9208
$2_1^+ \rightarrow 4_1^+$	$1.2671 \pm 0.1193$	2.3668
$4_1^+ \rightarrow 6_1^+$	$0.7222 \pm 0.1824$	0.0004
$0_1^+ \rightarrow 2_2^+$	$0.0780 \pm 0.0150$	0.0087
$0_1^+ \rightarrow 2_3^+$	$0.0445 \pm 0.0055$	0.0393
$0_1^+ \rightarrow 2_4^+$	$0.0755 \pm 0.0075$	0.0021
$0_1^+ \rightarrow 2_5^+$	$0.0073 \pm 0.0020$	0.0026
$0_1^+ \rightarrow 2_6^+$	$0.0130 \pm 0.0040$	0.0004
$0_1^+ \rightarrow 2_7^+$	$0.0355 \pm 0.0150$	0.0082
$0_2^+ \rightarrow 2_1^+$	$0.4343 \pm 0.0808$	0.0006
$0_2^+ \rightarrow 2_2^+$	$0.1765 \pm 0.0760$	4.9371
$0_2^+ \rightarrow 2_4^+$	$0.5050 \pm 0.5810$	0.0001
$0_2^+ \rightarrow 2_5^+$	$1.3890 \pm 0.3280$	0.0016
$0_2^+ \rightarrow 2_7^+$	$0.0757 \pm 0.0430$	0.0001
$0_2^+ \rightarrow 2_9^+$	$0.0255 \pm 0.0125$	0.0001
$0_3^+ \rightarrow 2_1^+$	$0.0227 \pm 0.0035$	0.0042
$0_4^+ \rightarrow 2_1^+$	$> 0.0019$	0.0025
$2_1^+ \rightarrow 4_4^+$	$0.0007 \pm 0.0001$	0.0031
$2_2^+ \rightarrow 4_4^+$	$0.0202 \pm 0.0045$	0.0004
$2_3^+ \rightarrow 4_3^+$	$0.9825 \pm 0.1653$	0.1358
$2_4^+ \rightarrow 4_1^+$	$0.1212 \pm 0.0138$	0.0001
$2_4^+ \rightarrow 4_4^+$	$2.2037 \pm 0.4591$	0.0049
$2_5^+ \rightarrow 4_1^+$	$0.0734 \pm 0.0274$	0.0013
$2_7^+ \rightarrow 4_1^+$	$0.0146 \pm 0.0066$	0.0002
$2_9^+ \rightarrow 4_1^+$	$0.0197 \pm 0.0081$	0.0001
$2_4^+ \rightarrow 4_6^+$	$0.1212 \pm 0.0252$	0.1705

Table 11: B(E2) transition strengths for  $^{28}\text{Si}$  ( $[e^2b^2 \times 10^{-2}]$  with  $q_{eff}$  is 1.3.)

go like cubic powers of  $\lambda$  and  $\mu$  [23], being in general large numbers. For this reason its coefficient was selected to be very small:  $4.64 \times 10^{-4}$ . Its effect on the wavefunction can be appreciated in Figure 8. It drives irreps with  $\mu \gg \lambda$  lower in energy than those with  $\mu \ll \lambda$ . As this is a mid-shell nucleus so it has the same number of particles and holes, it has two bands originated from the (12,0) and (0,12) irreps which would be degenerated for a pure quadrupole-quadrupole interaction. A similar feature has been found in Hartree-Fock calculations, where two minima coexist [35]. It was shown that the  $l \cdot s$  single particle term breaks this degeneracy and favors the dominance in the ground state band of the (0,12) irrep [35]. But the  $l \cdot s$  term alone is unable to push the first excited  $0^+$  state to an energy of 4.98 MeV. We found that, at most, it breaks the degeneracy putting this state at 1.16 MeV. A similar trend is observed in other states belonging to the first excited (prolate) band. The term proportional to  $C_3$  allows us to put the first excited  $0^+$  at the correct energy, as can be seen in Figure 7. With this Hamiltonian we obtain a very good description of this nucleus. Some states ( $1_1$ ,  $2_3$ ,  $2_4$  and  $5_1$ ) deviate from the experimental values in a way that is similar to those predicted by shell-model calculations [31, 32].

In Figure 8 the crossing of the oblate [(0,12),(1,10)] and prolate [((12,0), (10,1))] bands can be seen, which is a special feature of this mid-shell nucleus. With the  $C_3$  term in the Hamiltonian, the crossing in Figure 8 insert a) occurs at  $J = 6$ , while without this term, insert b), it occurs at  $J = 4$ . This happens because  $C_3$  favors the  $J = 4$  state belonging to the (0,12) band, driving it lower in energy than its counterpart from (12,0). Without  $C_3$  there is a state with  $J = 4$  at 4.58 MeV dominated by the (0,12) irrep, as for the calculation with  $C_3$ , but in this case there is another  $J = 4$  state dominated by the (12,0) irrep at 2.87 MeV.

As it was the case for lighter nuclei, the energy spectra is reproduced fairly well, and the quality of the results is comparable with those obtained by Wildenthal and Endt [31, 32] with a full shell-model calculation. The ground state band and many excited states are properly described. Given that this nucleus lies exactly at mid-shell, it is the most complex even-even nuclei of the sd shell. The presence of a  $3_1^+$  state that is lower in energy than the  $2_2^+$  state, i.e. which does not belong to the  $\gamma$  band, is impossible to understand within the context of the present model, while shell-model calculations reproduce this state. Similar problems occur for other excited states, like the  $2_3^+$ ,  $6_2^+$ ,  $6_3^+$ .

In Table 11 the B(E2) transition strengths are shown. While there are

many measured transitions, mostly of them involve the  $0^+$ ,  $2^+$  and  $4^+$  states. The agreement between theory and experiment is not as good as in the other nuclei, but shows the same trend found in full shell-model calculations for  $^{28}\text{Si}$ . There are few B(E2) experimental intensities with large strength, they allow us to identify some bands like those formed by the set of states  $(0_1^+, 2_1^+, 4_1^+, 6_1^+)$ ;  $(2_2^+, 4_3^+)$  and  $(2_4^+, 4_4^+)$ . On other hand, theoretical strengths suggest the following associations between positive parity states:  $(0_1, 2_1, 4_1, 6_3, 8_5)$ ;  $(0_2, 2_2, 4_2, 6_2, 8_1, 10_1)$ ;  $(0_3, 2_3, 4_6, 6_7, 8_{11}, 10_6)$ ;  $(0_4, 2_6, (4_7, 4_9))$ , where a couple of states with  $J = 4$  in parentheses means that there are large strengths toward both states.

## 7 Conclusions

The quasi SU(3) symmetry concept, first introduced in full shell-model calculations, was used in this work to explore the structure of four even-even sd-shell nuclei. While the SU(3) symmetry of these nuclei has been used since 1959, the new feature in this work is a close look at the role of proton and neutron irreps with spin  $S=1$ . It turns out that these configurations make large, often dominant contributions to the structure of members of the ground-state band, especially those states with higher angular momentum values.

The energy spectra and B(E2) transition strengths of  $^{20,22}\text{Ne}$ ,  $^{24}\text{Mg}$  and  $^{28}\text{Si}$  were calculated in a truncated basis based on the quasi SU(3) symmetry. A simple Hamiltonian which contains realistic single-particle energies, pairing and quadrupole-quadrupole terms was used. Both, the energy spectra and B(E2) transition were found to be very close to the corresponding experimental values. For the  $^{20,22}\text{Ne}$  cases the calculations were performed in the complete as well as a quasi SU(3) truncated basis, allowing for a discussion of the benefits and limitations of the truncation scheme. While including a few SU(3) irreps in the basis is enough to obtain good description of deformed nuclei, irreps with spin 1 and 2 and largest  $C_2$  values must be present. Effects of the three rotor-like terms in the Hamiltonian were discussed in detail for the  $^{24}\text{Mg}$  case.

The results of this work re-enforce the claim that the quasi SU(3) symmetry is a very powerful concept, raising expectations for its use in a description of intruder states in heavy deformed nuclei. Together with a pseudo SU(3) description for nucleons in normal parity states in these nuclei, one can antic-

ipate a relatively simple  $SU(3)$  description (pseudo for normal parity orbitals and quasi for intruders) of heavy deformed nuclei which has been missing up to now.

## 8 Acknowledgements

This work was supported in part by Conacyt (México) and the National Science Foundation under Grant PHY-9970769 and Cooperative Agreement EPS-9720652 that includes matching from the Louisiana Board of Regents Support Fund.

## References

- [1] A. P. Zuker, J. Retamosa, A. Poves, and E. Caurier, *Phys. Rev. C* **52**, R1741 (1995).
- [2] G. Martínez-Pinedo, A. P. Zuker, A. Poves, and E. Caurier, *Phys. Rev. C* **55**, 187 (1997).
- [3] C. E. Vargas, J. G. Hirsch, P. O. Hess, and J. P. Draayer, *Phys. Rev. C* **58**, 1488 (1998).
- [4] J. P. Elliott, *Proc. Roy. Soc. London Ser. A* **245**, 128 (1958); **245**, 562 (1958).
- [5] A. Arima, M. Harvey, and K. Shimizu, *Phys. Lett. B* **30**, 517 (1969).
- [6] J. P. Draayer, K. J. Weeks, and K. T. Hetch, *Nucl. Phys. A* **381**, 1 (1982).
- [7] J. P. Draayer, and K. J. Weeks, *Ann. Phys.* **156**, 41 (1984).
- [8] O. Castaños, J. P. Draayer, and Y. Leschber, *Ann. Phys.* **180**, 290 (1987)
- [9] O. Castaños, J. P. Draayer, and Y. Leschber, *Z. Phys* **329**, 33 (1988).
- [10] C. Bahri and J. P. Draayer, *Comput. Phys. Commun.* **83**, 59 (1994).
- [11] D. Rompf , T. Beuschel, J. P. Draayer, W. Scheid, and J.G. Hirsch, *Phys. Rev. C* **57**, 1703 (1998).

- [12] T. Beuschel, J. P. Draayer, D. Rompf , and J.G. Hirsch, Phys. Rev. **C 57**, 1233 (1998).
- [13] T. Beuschel, J. G. Hirsch, J. P. Draayer, Phys. Rev. **C 61**, 54307 (2000).
- [14] C. E. Vargas, J. G. Hirsch, T. Beuschel, and J. P. Draayer, Phys. Rev. **C 61** 031301(R)
- [15] C. E. Vargas, J. G. Hirsch, and J. P. Draayer, Nucl. Phys.**A 673**, 219 (2000).
- [16] J. Escher, J. P. Draayer, and A. Faessler, Nucl. Phys. A **586**, 73 (1995).
- [17] E. Caurier, J. L. Egidio, G. Martínez-Pinedo, A. Poves, J. Retamosa, L. M. Robledo, and A. P. Zuker, Phys. Rev. Lett. **75**, 2466 (1995).
- [18] J. G. Hirsch, P. O. Hess, C. E. Vargas, L. Hernández, T. Beuschel and J. P. Draayer. Rev. Mex. Fis. **45** Supl. 2, 86 (1999).
- [19] C. E. Vargas, J.G. Hirsch, and J.P. Draayer, Nucl. Phys. **A** in preparation.
- [20] M. Moshinsky, *Group Theory and the Many body Problem* (Gordon and Breach, New York, 1967).
- [21] J. P. Draayer in *Algebraic Approaches to Nuclear Structure* ed. by R. F. Casten *et al.*, (Harwood Academic Publishers, 1993).
- [22] C. Bahri, J. Escher, and J. P. Draayer, Nucl. Phys. A **592**, 171 (1995); **594**, 485 (1995).
- [23] D. Troltenier, C. Bahri, and J. P. Draayer, Nucl. Phys. A **586**, 53 (1995); **589**, 75 (1995).
- [24] D. Troltenier, J. P. Draayer, and J. G. Hirsch, Nucl. Phys. A **601**, 89 (1996).
- [25] P. Ring and P. Schuck. *The Nuclear Many-Body problem*, Springer, Berlin, 1979.
- [26] M. Dufour and A. P. Zuker, Phys. Rev. C **54**, 1641 (1996).

- [27] H. A. Naqvi and J. P. Draayer, Nucl. Phys. A **516**, 351 (1990); **536**, 297 (1992).
- [28] Y. Leschber, Hadronic Journal Supplement **3**, 1 (1987).
- [29] National Nuclear Data Center, <http://bnlnd2.dne.bnl.gov>
- [30] B. M. Freedom and B. H. Wildenthal, Phys. Rev. C **6** (1972) 1633.
- [31] B. H. Wildenthal, Prog. Part. Nucl. Phys. **11**, 5 (1984) and B. A. Brown, W. A. Richter, K. E. Julies, and B. H. Wildenthal, Ann. Phys. **182**, 191 (1988).
- [32] P. M. Endt, C. Alderliesten, F. Zijderhand, A. A. Wolters, and A. G. M. Van Hees, Nucl. Phys. A **510**, 209 (1990).
- [33] C. W. Johnson, V. G. Gueorguiev, J. P. Draayer, private communication.
- [34] E. Caurier, J. L. Egido, G. Martínez Pinedo, A. Poves, J. Retamosa, L. M. Robledo and A. P. Zuker, Phys. Rev. Lett. **75**, 2466 (1995).
- [35] S. Das Gupta, and M. Harvey, Nucl. Phys. A **94**, 602 (1967).